

# Psychoacoustic Aspects of Helicopter Sounds

Hugo Fastl<sup>1</sup>, Jakob Putner<sup>1</sup>, Jae Hun You<sup>2</sup>, Christian Breitsamter<sup>2</sup>, Philipp Krämer<sup>3</sup>

<sup>1</sup> AG Technische Akustik, MMK, TU München, 80333 München, Germany, Email: fastl@mmk.ei.tum.de

<sup>2</sup> Lehrstuhl für Aerodynamik und Strömungsmechanik, 85748 Garching, Germany

<sup>3</sup> Eurocopter Deutschland GmbH, 81663 München, Germany

## Introduction

In the framework of the research network FORLärm, psychoacoustic aspects of helicopter sounds are studied. The partner from industry is Eurocopter, and from Technische Universität München, the Institute of Aerodynamics and Fluid Mechanics as well as the AG Technical Acoustic are involved.

As a first topic of the cooperation, the noise produced by a shrouded tail rotor of a helicopter (Fenestron®) is assessed. Based on problem specifications by Eurocopter, Unsteady Reynolds Averaged Navier-Stokes (URANS) simulations are performed at the Institute of Aerodynamics and Fluid Mechanics. The calculations are carried out on a structured mesh with minimum simplification to calculate the flow field around and in the Fenestron®. To compute the sound pressure in the acoustic far field, the Ffowcs Williams and Hawkings (FW-H) surface integral formulation was adopted [4, 5]. After comprehensive simulations, 170 ms of time-signal were obtained by the aeroacoustic calculations.

These signals were further processed by the Technical Acoustics group. First, they were looped in order to enable informal listening tests and the analysis by algorithms, based on the results of psychoacoustic experiments. Then distributions of instrumental loudness were calculated and analysed in terms of hearing sensations.

In this paper, data are discussed in view of the loudness and sharpness of the simulated helicopter sounds at different spatial positions.

## Aerodynamic Studies

Conventional helicopter configurations (single main and tail rotor) feature a tail rotor in order to compensate for the main rotor torque and to provide flight control around the yaw axis. There are two design concepts of the tail rotor: open tail rotor and encapsulated tail rotor, also called Fenestron®.

The encapsulated tail rotor is normally a one-stage (rotor and stator) fan, embedded in the helicopter vertical fin (cf. Figure 1). The shrouding concept of rotor blades with duct fairing provides various benefits in contrast to the open tail rotor configuration.

First of all, the duct fairing ensures peripheral protection of rotor blades. From an acoustic point of view, the duct fairing acts as an acoustic shield, in particular for the sound radiation in the plane of rotation. Furthermore, the rotor blades of the Fenestron® are unevenly distributed in the circumferential direction to modulate dominant shrill noise related to the discrete noise at blade passing frequency (BPF) and corresponding harmonics.

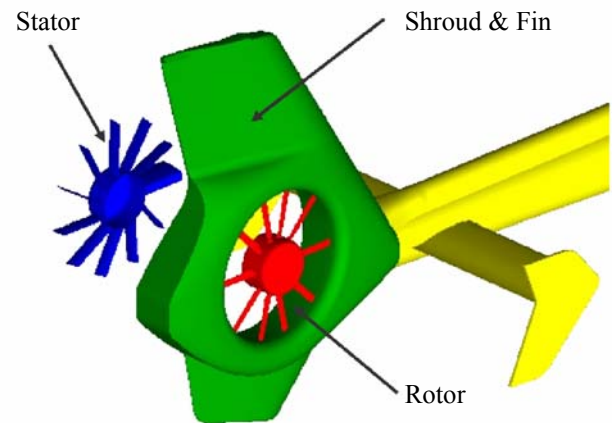


**Figure 1:** Fenestron® configuration (perspective from the fan inlet side).

Taken as a whole, the Fenestron® is regarded quieter than the conventional open tail rotor.

However, particularly in forward flight condition, the surrounding construction can provoke undesirable flow phenomena (e.g. inlet flow distortion), which could have a negative impact on the acoustic properties of the Fenestron®. In this context, a detailed understanding of noise generation mechanism of the Fenestron® is still required.

Therefore, numerical aeroacoustic calculations were performed for a full scale light weight transport helicopter including the Fenestron®. Hereby, an acoustic hybrid approach combining computational fluid dynamics (CFD) and aeroacoustic analogy were employed. Since this method treats computing of aerodynamic sound sources in the near-field and linear propagation into the far-field separately, it allows establishing the noise level with assessable computational costs for such a very complex configuration.

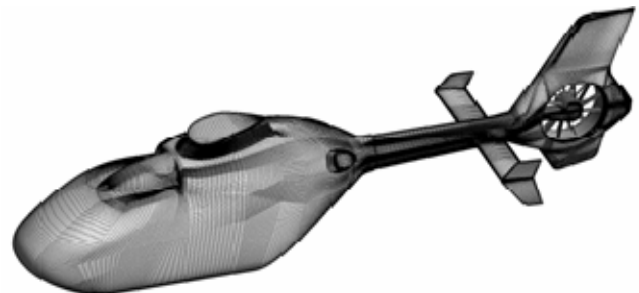


**Figure 2:** Surface mesh on the helicopter configuration (perspective from the fan outlet side).

The hybrid approach applied here is as follows: As a first step, the unsteady viscous flow field in the source regions is computed by using URANS simulations with Shear Stress Transport (SST) turbulence model. For this purpose, a multi-block structured mesh is generated on the helicopter configuration with minimum simplification (cf. Figure 2). A constant numerical time step corresponding to one degree of rotation of the blades is used for the whole unsteady computation. Transient samples, which contain the information about pressure, density and velocity field in the aerodynamic source regions, are collected every three time steps, leading to a total of 1200 samples for 10 fan revolutions.

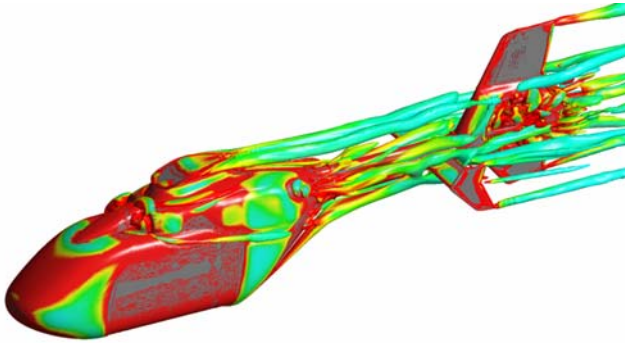


**Figure 3:** Instantaneous vortical structures visualized by means of isosurface of Q-criterion ( $Q = 2000 \text{ 1/s}^2$ ). Isosurface is coloured by dimensionless vorticity ( $\Omega_{\max} = 5$ )

As illustrated in Figure 3, the results of URANS computations reveal that in forward flight, the Fenestron® operates under highly distorted flow conditions leading to the generation of sound. It results, on the one hand from the turbulent fluctuations caused by the vortical structures arising from flow separation on the helicopter after body, and on the other hand from the flow separation on the inlet-lip.

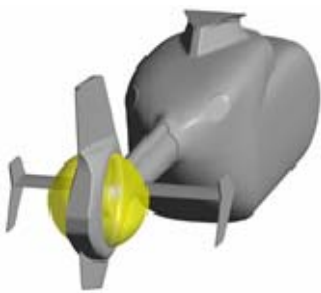


**Figure 4:** Control surfaces used for integrating Ffowcs Williams and Hawkins (FW-H) equation.

Based on the information gathered from the CFD task, aeroacoustic calculations were performed by applying the FW-H surface integral method. Hereby, the propagation of sound from the source region into the far-field is established by integration of the FW-H formulation on a control surface, on which the acoustic sources are allocated. Thus, two disconnected hemispherical control surfaces located on the fan inlet and outlet, respectively, are considered in the present study (cf. Figure 4).

The propagated sound pressure is then calculated at observer points with an equivalent distance (18 m) to the Fenestron®, but in different azimuthal angles, in order to determine the directivity of the Fenestron® noise (cf. Figure 5).

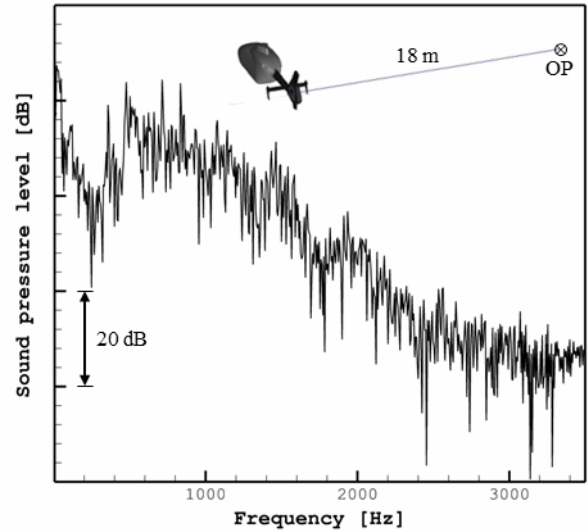


**Figure 5:** Sound pressure level as a function of frequency as calculated by the FW-H method for an observer point located at the fan inlet side ( $270^\circ$ ) in a distance of 18 m.

## Psychoacoustic Aspects

As described in detail in the section “Aerodynamic Studies”, helicopter tail rotor noises at eight positions in equal distance (18 m) of the tail rotor and different angles to the helicopter were simulated by the aeroacoustics group. Due to the high computation effort, the calculated helicopter tail rotor noise signal had a total duration of only 170 ms. For detailed psychoacoustic evaluations this signal duration is too short. Therefore, the signal duration was extended by subsequent processing steps. The 170 ms signal periods were looped in order to extend the overall signal duration to 10 s. Beginning and end of each signal period overlapped for 10 ms and were mixed with a Gaussian shaped crossfade in order to prevent audible clicks. This processing influences the frequency spectrum because of the periodicity of the looped signal, but the spectral envelope is preserved. Hence, such a procedure seems to represent a reasonable compromise in order to avoid exorbitant calculation times for the simulations.

Using the procedure of magnitude estimation (e.g. Fastl and Zwicker 2007 [3]), in an informal listening test the processed signals were evaluated, and distinct differences in loudness and timbre of the noises at various positions around the tail rotor were found.

Noises at the positions on axis of the tail rotor are perceived considerably louder than noises in front or behind the tail rotor. This behaviour is also reflected in the instrumental loudness analysis according to DIN 45631/A1 [1]. Corresponding loudness values are given in Table 1, and illustrated in Figure 6.

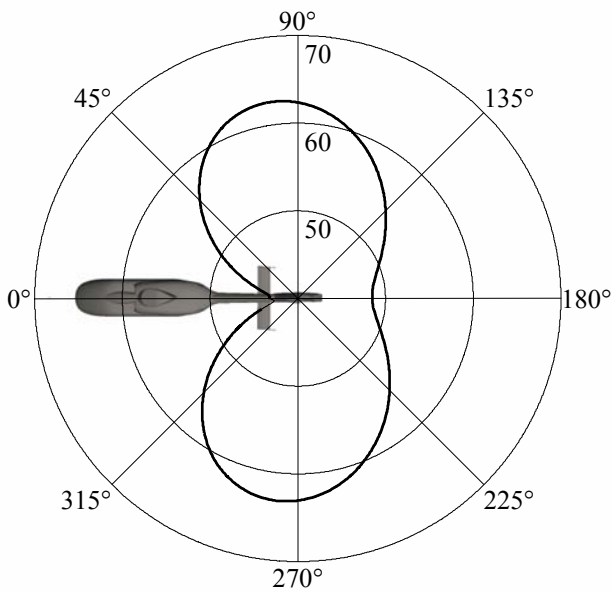


**Figure 6:** Loudness of the simulated noise around the helicopter tail rotor at a distance of 18 m.

Angle	Loudness
0°	43.31 sone
30°	50.23 sone
90°	62.18 sone
150°	51.96 sone
180°	47.13 sone
210°	52.41 sone
270°	62.86 sone
330°	49.11 sone

**Table 1:** Loudness of the simulated noise around the helicopter tail rotor at a distance of 18 m.

The results plotted in Figure 6 show a distinct directivity pattern of the loudness of the helicopter tail rotor noise. As already observed in the listening tests, the loudness on axis of the tail rotor (90° and 270°) is higher than the loudness at the other positions around the helicopter. Compared to the front (0°) the loudness at the sides (90° and 270°) is almost 50% higher.

Differences in the timbre of the noises were also observed during the informal listening tests. For example the noise behind the helicopter sounds somewhat more muffled and less sharp than the noise in front of the helicopter.

These perceptual differences are reflected in the instrumental sharpness values calculated according to DIN 45692 [2] and listed in Table 2.

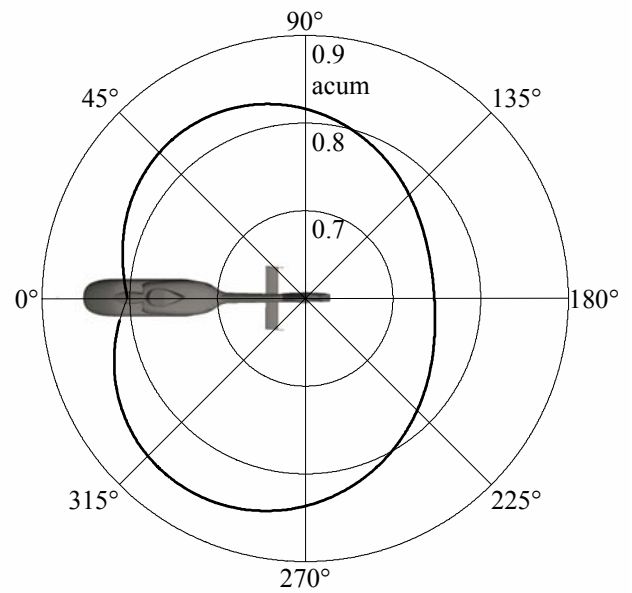


**Figure 7:** Sharpness of the simulated noise around the helicopter tail rotor at a distance of 18 m.

Angle	Sharpness
0°	0.80 acum
30°	0.83 acum
90°	0.82 acum
150°	0.75 acum
180°	0.76 acum
210°	0.76 acum
270°	0.84 acum
330°	0.84 acum

**Table 2:** Sharpness of the noise around the helicopter tail rotor at a distance of 18 m.

The directivity pattern of the instrumental sharpness of the noise around the helicopter tail rotor is given in Figure 7. It shows somewhat (~10%) higher sharpness values for the noises at the helicopter front than for the noises at the helicopter tail.

Loudness patterns as shown in Figures 8-11 clearly illustrate the differences in loudness and timbre of the noises at the various positions around the helicopter tail rotor. When comparing Figure 8 and 9, the loudness differences of about 50% are clearly reflected in the different areas below the curves.

The noise behind the helicopter (180°), which sounds somewhat more muffled and about 10% less sharp, has higher specific loudness values in the lower critical-bands, as shown in Figure 10, than the noise in front of the helicopter (0°), shown in Figure 8.

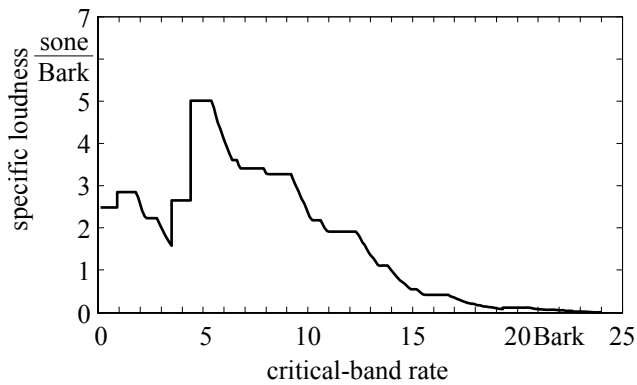


**Figure 8:** Loudness pattern of the helicopter tail rotor noise at the 0° position of the helicopter.

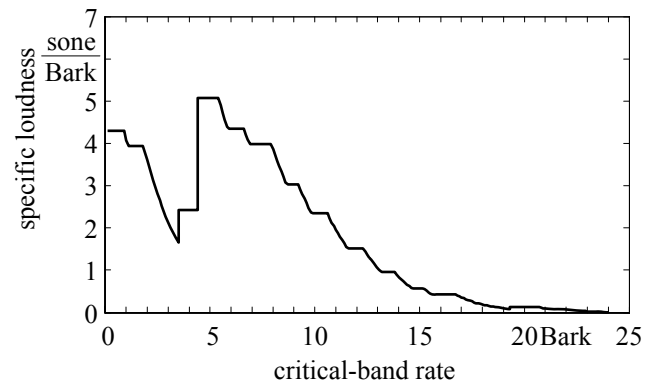


**Figure 10:** Loudness pattern of the noise at the 180° position of the helicopter.

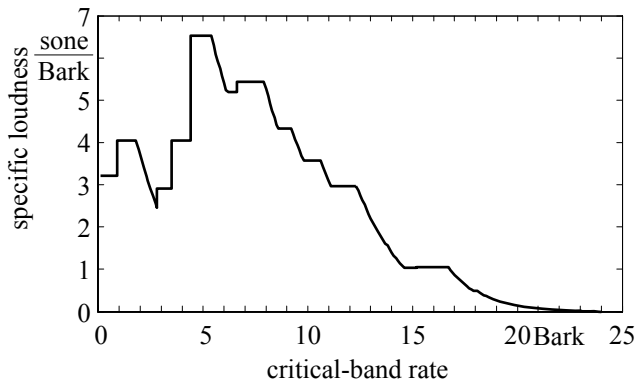


**Figure 9:** Loudness pattern of the helicopter tail rotor noise at the 90° position of the helicopter.

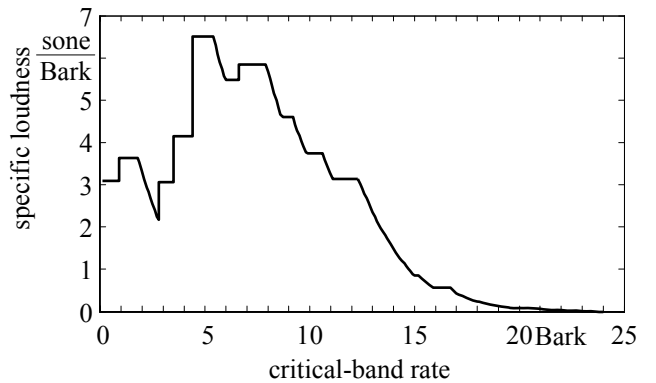


**Figure 11:** Loudness pattern of the noise at the 270° position of the helicopter.

High values of specific loudness can be seen around 5 Bark in all loudness patterns, for positions on and off axis of the tail rotor. The observed higher overall loudness for the on axis positions can be explained by the increase of the specific loudness at 5 Bark and in higher critical-bands especially around 7 Bark.

## Conclusions

Perceived differences in loudness and timbre of simulated noises at a distance of 18 m around the (shrouded) tail rotor of a helicopter (Fenestron®) can be assessed by instrumental evaluations according to DIN 45631/A1 and DIN 45692. The corresponding loudness patterns represent a spectral analysis according to features of the human hearing system. Therefore, they can give guidelines for further improvement of the radiated noise not only in physical terms but also in terms of perception. Eventually, loudness patterns also can give hints with respect to the acceptance of noises by the public.

## Acknowledgments

This research was supported by the Bavarian Research Foundation as part of the FORLärm research cooperation for noise reduction in technical equipment.

## References

- [1] DIN 45631/A1: Berechnung des Lautstärkepegels und der Lautheit aus dem Geräuschspektrum - Verfahren nach E. Zwicker - Änderung 1: Berechnung der Lautheit zeitinvarianter Geräusche. Beuth Verlag, Berlin (März 2010).
- [2] DIN 45692: Messtechnische Simulation der Hörempfindung Schärfe. Beuth Verlag, Berlin (August 2009).
- [3] Fastl H., E. Zwicker: Psychoacoustics. Facts and Models. 3rd Edition (Springer, Berlin, New York 2007)
- [4] You, J.H., Thouault, N., Breitsamter, C., Adams, N.A.: Aeroacoustic Analysis of a Helicopter Configuration with Ducted Tail Rotor, Proceedings of 28th Congress of the International Council of Aerospace Sciences, ICAS-2012-3:9.1, Brisbane (Sept. 2012).
- [5] You, J.H., Breitsamter, C.: Numerical Investigation of Aeroacoustic Sound Sources in Encapsulated Helicopter Tail Rotor, Proceedings of AIA-DAGA 2013, Meran (March 2013).